

The central role of mosquito cytochrome P450 CYP6Zs in insecticide detoxification revealed by functional expression and structural modelling

Alexia CHANDOR-PROUST*, Jaclyn BIBBY†, Myriam RÉGENT-KLOECKNER*, Jessica ROUX*, Emilie GUITTARD-CRILAT‡, Rodolphe POUPARDIN*§, Muhammad Asam RIAZ*||, Mark PAINE§, Chantal DAUPHIN-VILLEMANT‡¶, Stéphane REYNAUD* and Jean-Philippe DAVID*¹

*Laboratoire d'Ecologie Alpine (LECA), UMR 5553 CNRS, Université de Grenoble, Grenoble 38041, France, †Institute of Integrative Biology, University of Liverpool, Liverpool L69 7ZB, U.K., ‡Université Pierre et Marie Curie, CNRS, Paris 75005, France, §Liverpool School of Tropical Medicine, Liverpool L3 5QA, U.K., ||Department of Agri-Entomology, University College of Agriculture, University of Sargodha, Sargodha, Pakistan, and ¶Department of Ecology and Evolution, University of Lausanne, Lausanne 1015, Switzerland

The resistance of mosquitoes to chemical insecticides is threatening vector control programmes worldwide. Cytochrome P450 monooxygenases (CYPs) are known to play a major role in insecticide resistance, allowing resistant insects to metabolize insecticides at a higher rate. Among them, members of the mosquito CYP6Z subfamily, like *Aedes aegypti* CYP6Z8 and its *Anopheles gambiae* orthologue CYP6Z2, have been frequently associated with pyrethroid resistance. However, their role in the pyrethroid degradation pathway remains unclear. In the present study, we created a genetically modified yeast strain overexpressing *Ae. aegypti* cytochrome P450 reductase and CYP6Z8, thereby producing the first mosquito P450–CPR (NADPH-cytochrome P450-reductase) complex in a yeast recombinant system. The results of the present study show that: (i) CYP6Z8 metabolizes PBA1c (3-phenoxybenzoic alcohol)

and PBA1d (3-phenoxybenzaldehyde), common pyrethroid metabolites produced by carboxylesterases, producing PBA (3-phenoxybenzoic acid); (ii) CYP6Z8 transcription is induced by PBA1c, PBA1d and PBA; (iii) *An. gambiae* CYP6Z2 metabolizes PBA1c and PBA1d in the same way; (iv) PBA is the major metabolite produced *in vivo* and is excreted without further modification; and (v) *in silico* modelling of substrate–enzyme interactions supports a similar role of other mosquito CYP6Zs in pyrethroid degradation. By playing a pivotal role in the degradation of pyrethroid insecticides, mosquito CYP6Zs thus represent good targets for mosquito-resistance management strategies.

Key words: cytochrome P450 monooxygenase, insecticide, metabolism, mosquito, pyrethroid, recombinant system, resistance.

INTRODUCTION

Mosquitoes transmit numerous parasites and viruses responsible for severe human diseases, such as malaria or dengue. These diseases represent an important burden in tropical and subtropical regions, predominantly affecting developing countries [1]. Indeed, half of the world's population is at risk of malaria, whereas dengue represents a major threat in over 100 countries with more than 2.5 billion people at risk [1].

In the absence of efficient treatments or vaccines, vector control often represents the most effective means for limiting disease transmission [2]. Effective vector control largely relies on the use of insecticides targeting adults or larvae [3] and, because of their high efficiency and cheapness, chemical insecticides remain the first line of defence against mosquitoes when disease prevalence is high. Chemical insecticides used for mosquito control belong to various chemical families, from which pyrethroids are mainly used for impregnating bednets and spraying.

However, resistance of mosquitoes to insecticides is threatening vector control programmes worldwide [4]. Resistance can be the consequence of a mutation of the protein targeted by the insecticide (target-site resistance), a lower penetration or a sequestration of the insecticide, or an increased biodegradation of the insecticide (metabolic resistance) [5,6]. Detoxification enzymes such as cytochrome P450 monooxygenases (P450s or CYPs), GSTs and CCEs (carboxy/choline esterases) are known for their roles in insecticide metabolism in insects [7,8] and their

overproduction has been frequently associated with resistance to chemical insecticides in mosquitoes [5,6].

P450s are haem-thiolate-containing enzymes present in almost all organisms and are involved in the metabolism of a wide range of molecules [9]. Most P450s involved in detoxification processes are expressed in the endoplasmic reticulum and catalyse the oxidation of xenobiotics or endogenous compounds in the presence of their obligatory electron donor CPR (NADPH-cytochrome P450-reductase) and sometimes Cyt b5 (cytochrome b5) [10]. Insect P450s are involved in metabolic resistance to various insecticides [7,9,11,12]. In mosquitoes, P450s are encoded by more than 100 CYP genes [13,14].

Following the development of transcriptomic tools in mosquitoes [14,15], several P450s overtranscribed in pyrethroid-resistant mosquitoes were identified [5,6]. Some of them have been validated as pyrethroid metabolizers such as *Anopheles gambiae* CYP6M2 and CYP6P3 [16,17], *Anopheles funestus* CYP6P9b [18] and *Aedes aegypti* CYP9J32 [19]. Among mosquito P450s, members of the CYP6Zs have been frequently associated with pyrethroid resistance [15,20–22]; however, this is not supported by functional studies as they do not appear to metabolize pyrethroids. Chiu et al. [23] showed that *An. gambiae* CYP6Z1 metabolized DDT, whereas pyrethroid metabolism was not mentioned. McLaughlin et al. [24] revealed that *An. gambiae* CYP6Z2 metabolized various substrates, but not pyrethroids. In *Ae. aegypti*, CYP6Z8 was found to be induced by insecticides and pollutants [22,25–28] and constitutively overtranscribed in

Abbreviations used: AeCPR, *Aedes aegypti* CPR; CPR, NADPH-cytochrome P450-reductase; Cyt b5, cytochrome b5; 7-OH, 7-hydroxycoumarin; PBA, 3-phenoxybenzoic acid; PBA1c, 3-phenoxybenzoic alcohol; PBA1d, 3-phenoxybenzaldehyde; qPCR, quantitative real-time PCR; R_t , retention time; SRS, substrate recognition site; TFA, trifluoroacetic acid.

¹ To whom correspondence should be addressed (email jean-philippe.david@ujf-grenoble.fr).

pyrethroid-resistant populations [14,29]. This gene was also found preferentially transcribed in tissues classically involved in insecticide metabolism such as midgut and Malpighian tubules [27].

In this context, the present study aimed at characterizing *Ae. aegypti* CYP6Z8 substrate selectivity and its ability to metabolize insecticides. For this purpose, a yeast expression system allowing the co-expression of any mosquito microsomal P450 along with its associated CPR was developed. Using this system, we obtained a functional microsomal membrane complex of CYP6Z8 and *Ae. aegypti* CPR, which was used for *in vitro* metabolism assays. Our data indicate that although CYP6Z8 metabolizes various substrates, it is not capable of metabolizing most insecticides. However, our data reveal that CYP6Z8 and CYP6Z2, an anopheline orthologue of CYP6Z8, are likely to play a pivotal role in the clearance of pyrethroid insecticides via further catabolism of pyrethroid derivatives obtained by the action of carboxylesterases. This is significant from an operational vector control perspective as it is the first direct evidence that secondary metabolism of insecticides pyrethroids by P450s is linked to resistance. *In silico* 3D-modelling of substrate–enzyme interactions supports the involvement of other mosquito CYP6Zs in this process. The findings of the present study are discussed in regard to metabolic resistance mechanisms and detoxification pathways in mosquitoes.

EXPERIMENTAL

Materials, strains and media

Enzymes were purchased from New England Biolabs, oligonucleotides were purchased from Eurogentec, chemicals were purchased from Sigma–Aldrich and culture media were purchased from Euromedex. DNA sequencing was performed by Cogenics (Genome Express). *Ae. aegypti* mosquitoes from the Bora-Bora strain were bred under standard insectary conditions as described in Poupardin et al. [22]. Yeast *Saccharomyces cerevisiae* strain W303-1B (*MAT α* ; *leu2*, *his3*, *trp1*, *ade2-1*, *ura3*, *can^R*, *cyr⁺*), henceforth known as W(N), represents the wild-type strain used for the construction of all other strains described in the present study and was kindly provided by Dr P. Urban and Dr D. Pompon (University of Toulouse, INSA-UPS-LISBP). SG(A)I synthetic minimum medium contained 20 g/l glucose (SGI), 1 g/l bactocasamino acids, 6.7 g/l yeast nitrogen base without amino acids and 40 mg/l DL-tryptophane. When required, 30 mg/l adenine was added (SGAI). N3 complete respiratory medium consisted of 10 g/l yeast extract, 10 g/l bacto-peptone and 2% glycerol. YPDA complete media contained 20 g/l glucose, 10 g/l yeast extract, 10 g/l bacto-peptone and 30 mg/l adenine. Repressive complete medium YPGE consisted of 5 g/l glucose, 10 g/l yeast extract, 10 g/l bacto-peptone and 3% ethanol. Solid media consisted of media described above with an addition of 20 g/l agar. All culture media were sterilized at 121 °C for 20 min before use.

Cloning and heterologous expression of *Ae. aegypti* Cyt b5

The full cDNA sequence of *Ae. aegypti* Cyt b5 (VectorBase accession number AAEL010017) was amplified by PCR using high-fidelity Taq Expand™ (Roche Applied Science) and the following primers: forward, 5'-ATGTCGGAAGTGAAAACCT-TCTCGC-3', and reverse, 5'-GTTAGCAGGTTACTGAGTAA-AGTAGAAC-3'. The amplification product was purified, cloned and sequenced. BamHI and EcoRI restriction sites were inserted

by PCR using the following primers: forward, 5'-AAGGATCC-AAAATGGCTGAAGTGAAAACC-3' (start codon underlined), and reverse, 5'-GCCGAATTCTTTACTGAGTAAAGTAGAAC-C-3'. The fragment was purified, cloned into the pET22b expression vector (Novagen) and resequenced. Protein expression was performed in *Escherichia coli* Rosetta 2 (DE3) cells as described previously [30]. Cyt b5 was then purified on a HiPrep DEAE–Sephacrose FF column (GE Healthcare) and eluted by a step gradient of NaCl. The fraction containing the purified Cyt b5 was then desalted using a HiPrep Desalting column (GE Healthcare) and concentrated using an Amicon Ultra YM10 filter unit (Millipore). High-molecular-mass contaminants were eliminated by using a HiLoad Superdex 75 column. Protein was concentrated again and purity was checked by SDS/PAGE. The Cyt b5 concentration was evaluated as described previously [31].

Cloning of CYP6Z8 and *Ae. aegypti* CPR for expression in yeast

The full cDNA sequence encoding *Ae. aegypti* CYP6Z8 (VectorBase accession number AAEL009131-RA) was amplified by PCR using high-fidelity Taq Expand™ (Roche Applied Science) and the following primers: forward, 5'-GCAAAGAGTT-CAAAATGGTCAT-3', and reverse, 5'-GCACAAGTTCTCTA-TTCAGC-3' (start and stop codons underlined). A similar procedure was used to amplify AeCPR (*Ae. aegypti* CPR; VectorBase accession number AAEL003349-RA) using the following primers: forward, 5'-ATGGACGCACAGACGGAAC-3', and reverse, 5'-TTTCAGCGGAGATGGATTAAC-3' (start and stop codons underlined). Both amplicons were fully sequenced and the corresponding synthetic gene was synthesized by GeneCust with optimization for yeast expression (codon usage, mRNA structure, GC content, and insertion of BamHI and EcoRI sites at 5' and 3' ends respectively).

Construction of CYP6Z8 and CPR expression plasmids

CYP6Z8 and CPR synthetic genes were subcloned into yeast replicative pYeDP60 and yeast integrative pYeDP110 plasmids (kindly provided by Dr P. Urban) as described in Pompon et al. [32]. Both vectors can be propagated in *E. coli*, hold an expression cassette under a glucose-repressed and galactose-inducible *GAL10-CYC1* promoter and included an *URA3* marker (uracil auxotrophy complementation). The plasmid pYeDP60 also contains an adenine *ADE2* marker. Both plasmids were digested with BamHI and EcoRI and purified with the Gel Extraction Purification kit (Qiagen). CYP6Z8 and CPR synthetic genes were ligated to pYeDP60 and pYeDP110 respectively using T4 DNA ligase and the ligation product was used to transform DH5 α chemically competent *E. coli*. Positive colonies were detected by PCR. Plasmids containing CYP6Z8 and CPR constructs were purified, double-digested and sequenced. Expression plasmids containing synthetic genes encoding CYP6Z8 and CPR were called pYeDP60-6Z8 and pYeDP110-CPR.

Stable integration of AeCPR into the yeast genome

The W(AeR) strain was obtained by stable integration of the AeCPR under the control of the *GAL10-CYC1* promoter into the W(N) genome. This genome integration was performed by disrupting the yeast CPR gene. Briefly, pYeDP110-CPR was first linearized by NotI and purified using a gel-extraction kit. Then, W(N) yeast were transformed as described previously using the lithium acetate/single-strand carrier DNA/PEG method [33] and spread on SGAI-agar plates. Positive colonies were streaked

individually on SGAI-agar plates, allowed to grow, and then streaked again on N3-agar plates to ensure they can grow in the absence of glucose (rho + phenotype). Positive colonies were checked by PCR to ensure the integrity of the recombined genomic locus.

Expression of CYP6Z8 in the W(AeR) yeast strain

W(AeR) yeast were transformed as described previously [33] by pYeDP60-6Z8. Positive colonies were streaked on SGI-agar plates and N3-agar plates and then checked by PCR to ensure the presence of the *CPR* gene and pYeDP60-6Z8 plasmid. Afterwards, 30 ml of stationary-phase SGI culture were used to inoculate 500 ml of YPGE and the culture was allowed to grow at 30°C for 48 h. When a D_{600} of 4 was reached, 20 g/l galactose was added to the culture to induce CPR and CYP6Z8 expression. The culture was further allowed to grow at 30°C for 7 h with horizontal agitation at 140 rev./min before microsome extraction.

Preparation of yeast CYP6Z8 microsomes

The culture was first centrifuged at 2000 g for 18 min and the pellet washed with 1 ml of TEK [50 mM Tris/HCl (pH 7.4), 1 mM EDTA and 100 mM KCl] per 0.5 g of cells. The pellet was resuspended in 10 ml of TES [50 mM Tris/HCl (pH 7.4), 1 mM EDTA, 0.6 M sorbitol, 1 mM PMSF and 1 mM DTT] and glass beads were added. Yeast cells were broken by vortex-mixing five times for 30 s at 4°C. TES (5 ml) was added to wash the beads and the supernatant was transferred into a clean tube. The beads were washed again twice, the supernatants pooled and centrifuged at 10000 g for 10 min. The supernatant was further ultracentrifuged at 27000 rev./min (rotor SW 28, Beckman Coulter) for 1 h. The pelleted microsomes containing CYP6Z8 and CPR were resuspended in 500 µl of TEG [50 mM Tris/HCl (pH 7.4), 1 mM EDTA and 30% glycerol] per 500 ml of yeast culture, aliquoted and stored at -80°C until use [32].

Quantification of CPR and CYP6Z8 in yeast microsomes

Microsomal protein concentration was determined using the Bradford method [34]. Specific content in P450s was measured from the reduced carbon monoxide difference spectra according to Omura and Sato [35] on both W(AeR)-CYP6Z8 microsomes and W(AeR) microsomes. CPR activities were measured in W(AeR)-CYP6Z8, W(AeR) and W(N) microsomes by following the reduction of cytochrome *c* at 550 nm, in the presence of NADPH [36].

Activity of CYP6Z8 microsomes against standard P450 substrates

Four resorufin ethers (methoxyresorufin, ethoxyresorufin, pentoxyresorufin and benzyloxyresorufin; Sigma-Aldrich) were tested as fluorogenic substrates against W(AeR)-CYP6Z8 microsomes. For each sample, 5 pmol of P450 in a total reaction volume of 200 µl was added to 0.1 M phosphate buffer (pH 7.4) containing 5 µM substrate, 0.1 mM NADPH and an electron regeneration system (3 mM glucose 6-phosphate and 0.4 unit of glucose-6-phosphate dehydrogenase), and incubated at 30°C for 60 min. The production of resorufin was monitored by measuring fluorescence at 537 nm excitation and 587 nm emission with a Varioskan Flash Multimode Reader (Thermo Fisher Scientific). A standard curve of resorufin (Sigma-Aldrich) was used to calculate product formation rate. 7-Ethoxycoumarin O-de-ethylation was

monitored in a similar manner. The reaction mix was identical as above, except that 8 pmol of P450 was used in a final volume of 100 µl. After 10, 30 and 60 min, the reaction was stopped by adding 100 µl of 50:50 (v/v) glycine/ethanol buffer and the production of 7-OH (7-hydroxycoumarin) was quantified by measuring the fluorescence at 380 nm excitation and 460 nm in comparison with an 7-OH standard (Sigma-Aldrich). The effect of the presence of Cyt b5 on CYP6Z8 activity was assessed by supplementing the incubation reaction with 2.5–50 pmol of Cyt b5. For the determination of kinetic parameters, the substrate concentration ranged from 0 to 10 µM and the incubation time was set to 15 min.

In vitro metabolism assays with non-fluorescent substrates

In vitro incubations contained 10 µM substrate, 50 pmol of *Ae. aegypti* CYP6Z8 in W(aeR) microsomes or AgCYP6Z2 in *E. coli* membranes [24] when indicated, 5 mM MgCl₂, 0.1 mM NADPH and the electron regenerative system (see above) for a total reaction volume of 100 µl. Control experiments consisted of omitting the NADPH regeneration system. After incubation at 30°C, the reaction was stopped by adding 100 µl of acetonitrile, shaking and incubation for 20 min and then centrifugation for 5 min at 16000 g to pellet microsomal proteins. The supernatant was then transferred into ultraclean glass vials and analysed by reverse-phase HPLC. The effect of the presence of Cyt b5 on CYP6Z8 activity was assessed by supplementing incubation mixtures with 80 pmol (8 equivalents) of purified *Ae. aegypti* Cyt b5.

Insecticide metabolism was monitored by reverse-phase HPLC on an Agilent 1260 HPLC system equipped with a Nucleodur C₁₈ Polartec 250 mm × 4.6 mm 3µ column (Macherey-Nagel) and a multi-wavelength photodiode array. Insecticides and potential metabolites were eluted with a gradient from 20 to 100% acetonitrile in water containing 0.1% TFA (trifluoroacetic acid) for 20 min, followed by a plateau at 100% for 4 min. For imidacloprid, a gradient from 10 to 50% acetonitrile in 20 min was used. Elution times of each compound and wavelengths used for their detection are shown in Table 1.

MS identification of PBAlc (3-phenoxybenzoic alcohol) metabolites

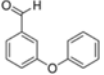
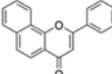
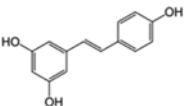
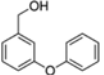
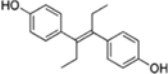
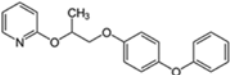
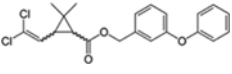
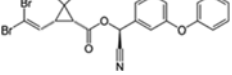
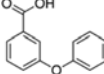
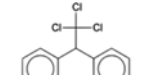
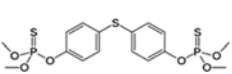
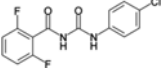
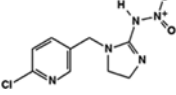
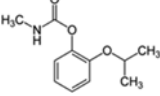
The LC-MS/MS analysis was performed on an Agilent 1100 HPLC coupled to a Bruker Esquire 3000+ Ion Trap mass spectrometer (Bruker Daltonics) in a positive mode (ESI+) under the following conditions: nebulizer gas 11 p.s.i. (N₂), drying gas 8 l/min, drying temperature 350°C, HV capillary 2000 V, HV End Plate Offset -500 V, capillary exit 103 V and skimmer 40 V.

In vivo metabolism assays

The ability of *Ae. Aegypti* third instar larvae to metabolize PBAlc and excrete metabolites was assayed by exposing third-stage larvae for 24 h to 10 µM PBAlc. In total, 25 larvae were exposed to 250 µl of PBAlc (10 µM) in open microcentrifuge tubes for 24 h under standard insectary conditions (26°C, 14 h/10 h light/dark period, 80% relative humidity). Controls consisted of a PBAlc solution without larvae and a PBAlc solution with larvae previously killed by heating at 95°C for 10 min. After 24 h, reactions were flash-frozen in liquid nitrogen, thawed and centrifuged at 13000 g for 1 min. Supernatant was then transferred into HPLC vials containing an equal volume of acetonitrile and subjected to HPLC analysis as described above to quantify remaining PBAlc and excreted metabolites.

Table 1 Metabolism of various xenobiotics by CYP6Z8

Turnover is measured as pmol of substrate depleted/min per pmol of P450. ND, not detected.

Substrate	Type	Turnover	Elution time (min); (wavelength, nm)	
	PBALd	Pyrethroid metabolite	1.978 ± 0.359	16.1 (232)
	α-Naphthoflavone (αNF)	Flavone	0.561 ± 0.022	19.1 (280)
	Resveratrol	Stilbene	0.463 ± 0.156	11.6 (300)
	PBAIc	Pyrethroid metabolite	0.425 ± 0.004	14.0 (232)
	Diethylstilbestrol	Stilbene	0.234 ± 0.072	18.3 (254)
	Pyriproxifen	Insecticide (growth regulator)	0.026 ± 0.001	18.7 (232)
	Permethrin	Insecticide (pyrethroid)	ND	22.0 and 22.4 (232)
	Deltamethrin	Insecticide (pyrethroid)	ND	21.4 (232)
	PBA	Pyrethroid metabolite	ND	15.9 (232)
	DDT	Insecticide (organochlorine)	ND	22.1 (232)
	Temephos	Insecticide (organophosphate)	ND	19.4 (232)
	Diflubenzuron	Insecticide (chitin synthesis inhibitor)	ND	16.7 (232)
	Imidacloprid	Insecticide (neonicotinoid)	ND	13.2 (270)
	Propoxur	Insecticide (carbamate)	ND	12.9 (232)

Induction of CYP6Z8 by hydrolysed pyrethroid metabolites

The induction of *CYP6Z8* by PBAIc, PBAld (3-phenoxybenzaldehyde) and PBA (3-phenoxybenzoic acid) was investigated by exposing third stage larvae for 24 h to 25, 250 and 2500 nM of each compound and measuring the

CYP6Z8 transcription level by reverse transcription followed by quantitative real-time PCR (RT-qPCR). Experimental procedures used for RNA extractions, reverse transcription, real-time PCR and primers used for qPCR are described in Poupardin et al. [27]. Data analysis was performed according to the $\Delta\Delta C_T$ method taking into account PCR efficiency [37] and using the

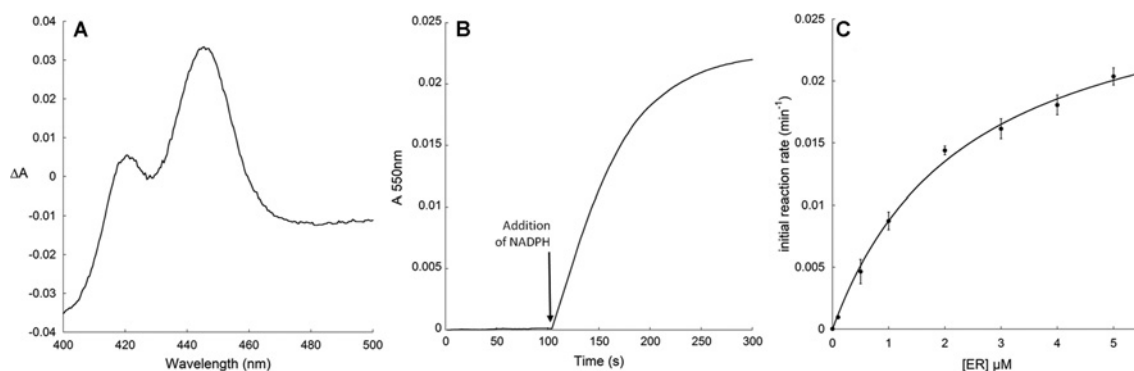


Figure 1 Biochemical characterization of yeast W(AeR)-CYP6Z8 microsomes

(A) Fe^{2+} -CO compared with Fe^{2+} difference spectrum. The spectrum was obtained from 1 mg of microsomal proteins containing 494 pmol of P450. (B) CPR activity of W(AeR) microsomes. Activity was quantified by monitoring the amount of reduced cytochrome *c* at 550 nm in the presence of NADPH and the NADPH regenerating system. (C) Michaelis–Menten plot of CYP6Z8–ethoxyresorufin (ER) kinetic parameters.

housekeeping gene encoding the ribosomal protein L8 (*AeRPL8*, GenBank[®] accession no DQ440262). Three independent biological replicates using different egg batches were performed and results were expressed as the mean transcription ratio relative to controls (unexposed larvae). Transcription data were computed by using a Mann–Whitney test on transcription ratios ($n = 3$). Genes were considered significantly overtranscribed compared with controls when the mean transcription ratio was superior to 1.5 and the Mann–Whitney *P* value was <0.05 .

In silico substrate docking 3D modelling

The molecular models of CYP6Z8 and other CYP6Zs were created based on the crystal structure of CYP3A4 ([38]; PDB code 1TQN), currently the most homologous protein with a known structure, with 28 % identity. Docking studies were carried out using GOLD v3.1 with the ChemScore scoring function [39] and an active site radius of 20 Å (1 Å = 0.1 nm). Ligand structures were obtained from ChemIDplus (<http://chem.sis.nlm.nih.gov/chemidplus/>). In total 50 binding modes were obtained for deltamethrin, PBA1c, PBA1d and PBA. Figures were prepared using PyMOL (<http://www.pymol.org>).

RESULTS

CYP6Z8 sequence analysis

Ae. aegypti CYP6Z8 was cloned from cDNA (Bora-Bora strain) and fully sequenced (*CYP6Z8v1*, GenBank[®] accession number JQ970488). Sequence analysis revealed 49 nucleotide variations compared with the genome sequence (gene AAEL009131, Liverpool strain, *AaegL1.2* genset) (Supplementary Figure S1 at <http://www.biochemj.org/bj/455/bj4550075add.htm>). Of these, 13 were non-synonymous, leading to 97.14 % identity with AAEL009131-PA (Supplementary Figure S2 at <http://www.biochemj.org/bj/455/bj4550075add.htm>). Only one non-synonymous variation was located within SRS (substrate recognition site) regions. This variation (C855A), leading to the replacement of a phenylalanine by a leucine at position 285 is not likely to affect substrate-binding properties. Indeed, structural models showed that this amino acid does not project into the active site and does not affect its dimensions. In addition, this variation was not predicted to affect the I helix position or substrate access channels (results not shown).

Creating a yeast strain overexpressing mosquito CPR

The W(N) yeast strain was submitted to homologous recombination with the integrative plasmid pYedP110-CPR to obtain the W(AeR) strain which overproduces AeCPR in the presence of galactose (*GAL* promoter). PCR with specific primers confirmed the stable replacement of the yeast *CPR* gene by the insert containing the *GAL* promoter and *AeCPR* gene. Microsomes extracted from galactose-induced W(AeR) cultures showed a significant overexpression of CPR activity compared with the W(N) strain (164 ± 49 nmol of reduced cytochrome *c*/min per mg of protein compared with 32 ± 13 nmol/min per mg of protein).

Co-expression of recombinant CYP6Z8 and CPR in yeast

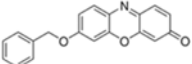
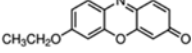
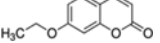
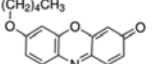
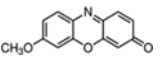
An average of 17 mg/l W(AeR)-CYP6Z8 microsomal proteins was obtained. The reduced CO-difference spectrum of W(AeR)-CYP6Z8 microsomes had a characteristic maximum absorption peak at 448 nm (Figure 1A). A minor peak was also observed at 420 nm (incorrectly folded protein), which increased to the detriment of the 450 nm peak for longer induction times, suggesting that CYP6Z8 is moderately stable. The average P450 concentration was 195 ± 51 pmol/mg. Endogenous expression of yeast P450s was not detectable in W(N) or W(AeR) microsomes. Finally, the expression of AeCPR ranged from 97 to 209 nmol of reduced cytochrome *c*/min (Figure 1B) and was not significantly affected by the co-expression of CYP6Z8.

CYP6Z8 activity against standard P450 fluorescent substrates

W(AeR) microsomes expressing only AeCPR did not show any significant activity against any P450 fluorescent substrate, confirming the very low expression of endogenous yeast P450s under these conditions. W(AeR)-CYP6Z8 microsomes were able to metabolize fluorescent substrates at different rates (Table 2 and Figure 1C). Determining apparent kinetic parameters, K_m and V_{max} , for each fluorescent substrate showed that CYP6Z8 metabolized preferentially ethoxyresorufin and benzyloxyresorufin (k_{cat}/K_m ratios of 0.49 and 0.74 respectively), whereas pentoxyresorufin and 7-ethoxycoumarin were metabolized at much lower rates (k_{cat}/K_m ratios of 0.0094 and 0.17 respectively). Apparent kinetic parameters for methoxyresorufin could not be determined due to a non-Michaelian behaviour of this substrate. Although Cyt b5 integration into W(AeR)-CYP6Z8 microsomes and its interaction with the P450 were observed (results not shown),

Table 2 CYP6Z8 specific activity against standard fluorescent P450 substrates

ND, not determined because of non Michaelis–Menten behaviour.

Substrate	K_m (μM)	V_{\max} (nM/min)	K_{cat} (min^{-1})	K_{cat}/K_m
	0.13 \pm 0.02	2.41 \pm 0.05	0.097 \pm 0.002	0.74
	2.39 \pm 0.28	30 \pm 1	1.19 \pm 0.05	0.49
	5.90 \pm 0.90	49 \pm 2	0.98 \pm 0.04	0.17
	13.96 \pm 3.14	3.29 \pm 0.02	0.13 \pm 0.01	0.0094
	ND	ND	ND	ND

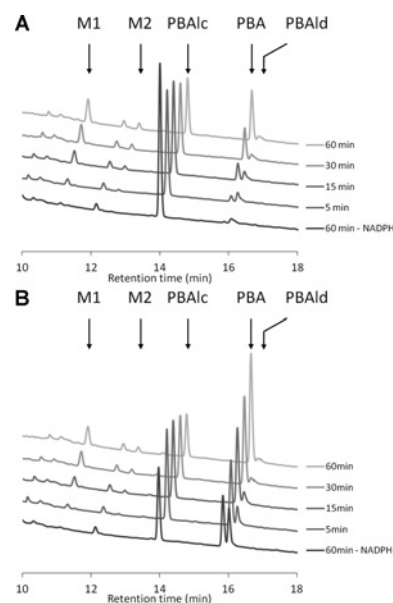
supplementing the reaction with recombinant Cyt b5 did not lead to a significant increase in activity for any of the substrates tested.

CYP6Z8 activity against insecticides and other xenobiotics

Metabolism of insecticides from various chemical classes was assayed with W(AeR)-CYP6Z8 microsomes in the presence or absence of NADPH and the NADPH regenerating system. The degradation of the substrate and appearance of metabolites were monitored by reverse-phase HPLC (Table 1). The insecticides permethrin, deltamethrin, DDT, temephos, diflubenzuron, imidacloprid and propoxur were not significantly metabolized by CYP6Z8. However, CYP6Z8 metabolized different natural and synthetic xenobiotics such as α -naphthoflavone, resveratrol, diethylstilbestrol and to a lesser extent the insecticide pyriproxyfen. As for fluorescent substrates, the presence of Cyt b5 did not affect CYP6Z8 substrate specificity and turnover (results not shown).

As pyrethroid catabolism may involve carboxylesterase-mediated hydrolysis as a first step, the conversion of intermediate metabolites, namely PBAIc and PBAId was also examined. When PBAIc was used as a substrate (Figure 2A), no significant metabolism occurred in the absence of NADPH and the NADPH regenerating system. In the presence of NADPH, PBAIc was metabolized by CYP6Z8 at a rate of 0.42 pmol/min per pmol of P450. PBAIc turnover was not significantly affected by the presence of Cyt b5 (results not shown). Several metabolites were produced by CYP6Z8 including PBA [R_t (retention time) 15.8 min], PBAId (R_t , 16 min) and two more hydrophilic metabolites, M1 and M2 (R_t , 11.1 min and 12.6 min respectively). PBA accumulated gradually and was the major metabolite after 60 min incubation, followed by the M1 metabolite. PBAId never accumulated to a large extent; its proportion increased progressively over 15 min before decreasing for longer incubation times, suggesting the further conversion of this metabolite. Finally, a minor M2 metabolite gradually appeared during incubation. Kinetic parameters of PBAIc metabolism were $K_m = 15.1 \pm 2.9 \mu\text{M}$, $V_{\max} = 33.4 \pm 1.5 \text{ pmol/min}$, $k_{\text{cat}} = 0.66 \pm 0.03 \text{ min}^{-1}$ and $k_{\text{cat}}/K_m = 0.046$.

When PBAId was used as a substrate (Figure 2B), a significant conversion into PBAIc occurred in the absence of CYP6Z8, suggesting that this reduction is CYP-independent. Conversion into PBA strongly increased in the presence of CYP6Z8 and

**Figure 2** Analysis of PBAIc and PBAId metabolism by CYP6Z8

HPLC chromatograms showing the time course of PBAIc (A) and PBAId (B) metabolism by W(AeR)-CYP6Z8 microsomes. The lowest off-set corresponds to the negative control (–NADPH) followed by reactions in the presence of NADPH stopped after 5, 15, 30 and 60 min. PBAIc, PBAId, PBA and metabolite peaks are indicated by arrows on the 60 min off-set.

NADPH (1.98 pmol/min per pmol of P450), confirming that CYP6Z8 also metabolizes PBAId. PBAIc remained a significant metabolite over time, indicating equilibrium between oxidation and reduction reactions. As for PBAIc, a minor production of M1 and M2 metabolites was noticed and PBAId turnover was not significantly affected by the presence of Cyt b5 (results not shown). Finally, no PBA metabolism occurred in the presence of NADPH, indicating that this compound is not further metabolized by CYP6Z8.

The ability of *An. gambiae* CYP6Z2, an anopheline orthologue of CYP6Z8, to metabolize PBAIc and PBAId was also investigated. These experiments performed with *E. coli* recombinant CYP6Z2 [24] under identical conditions demonstrated the ability of CYP6Z2 to metabolize both PBAIc and PBAId,

producing PBA together with minor M1 and M2 metabolites in the same way as CYP6Z8 (Supplementary Figure S3 at <http://www.biochemj.org/bj/455/bj4550075add.htm>).

Identification of metabolites

Positive-mode electrospray LC–MS detected PBAIc, PBAId, PBA, M1 and M2 at 183, 199, 215, 200 and 228 *m/z* respectively. PBAIc was detected 18 units below its theoretical mass (201 *m/z*), indicating its dehydration during LC–MS (Supplementary Table S1 at <http://www.biochemj.org/bj/455/bj4550075add.htm>). MS analyses did not allow the full identification of M1 and M2 metabolites. However, M1 and M2 metabolites did not appear to result from the direct or sequential hydroxylation of PBAIc or PBAId as no +16 *m/z* were observed. In addition, LC–MS *m/z* obtained for M1 and M2 did not match with any expected metabolite structure.

MS/MS analyses by positive-mode electrospray fragmentation detected various fragmentation ions associated with each compound (Supplementary Table S2 at <http://www.biochemj.org/bj/455/bj4550075add.htm>). The fragment shared by PBAId and PBA (171 *m/z*) is likely to correspond to diphenylether. This fragment could not be identified from M1 or M2, suggesting that these two metabolites rather originate from PBAIc. In addition, among all fragments, one was shared between PBAIc and M1 (155 *m/z*), suggesting a common backbone of these two compounds. This fragment was not shared with M2. Moreover, replacing H₂O/0.1% TFA (pH 2.0) by 10 mM Tris buffer (pH 7.5) for HPLC analysis resulted in the shift of PBA and PBAId peaks (results not shown), whereas PBAIc, M1 and M2 peaks were not affected (no change in signal intensity and *R_f*), suggesting that M1 and M2 do not possess any pH-dependent function, unlike PBAId or PBA.

In silico 3D modelling of CYP6Z–substrate interactions

In order to better understand why pyrethroids and their metabolites were metabolized or not by CYP6Zs, 3D models were built and the docking modes of PBAIc, PBAId, PBA and deltamethrin were predicted *in silico*. In CYP6Z8 and CYP6Z2, PBAId and PBAIc bound in two alternative modes that allow metabolism either on the phenyl or benzyl rings (Figure 3), consistent with experimental findings showing two metabolites. Given the phenyl ring structure of PBAId and PBAIc, interactions with aromatic side-chain amino acids are of potential interest in substrate binding and metabolism. A cluster of aromatic side chains are predicted in the active site of CYP6Z8, Phe¹⁰², Phe¹¹⁰, Phe¹¹⁵, Tyr²⁰⁸ and Phe²¹¹, of which Phe¹¹⁵ and Tyr²⁰⁸ appear to be positioned as clamps above the haem iron atom, thus potentially key residues in substrate positioning for catalysis (Figure 3). Orientation in two binding modes is predicted, consistent with the two products observed (PBAId and PBA). Despite their lack of deltamethrin metabolism, both CYP6Z8 and CYP6Z2 produced their highest binding scores with this compound (~42 kJ/mol) (Supplementary Table S3 at <http://www.biochemj.org/bj/455/bj4550075add.htm>). However metabolism appears to be prevented in CYP6Z8 by internal clashes with Tyr²⁰⁸, and in CYP6Z2 by residues close to the haem (Leu³⁶⁵ and Phe¹¹⁵). Steric hindrance of PBA does not appear to prevent metabolism since productive pose are predicted in CYP6Z8. However, the low binding score points to a low affinity for this molecule (Supplementary Table S3). Examination of structural models of other *Ae. aegypti* and *An. gambiae* CYP6Zs indicates they may all have the capacity to metabolize PBAIc and PBAId and produce similar metabolites (Figure 4).

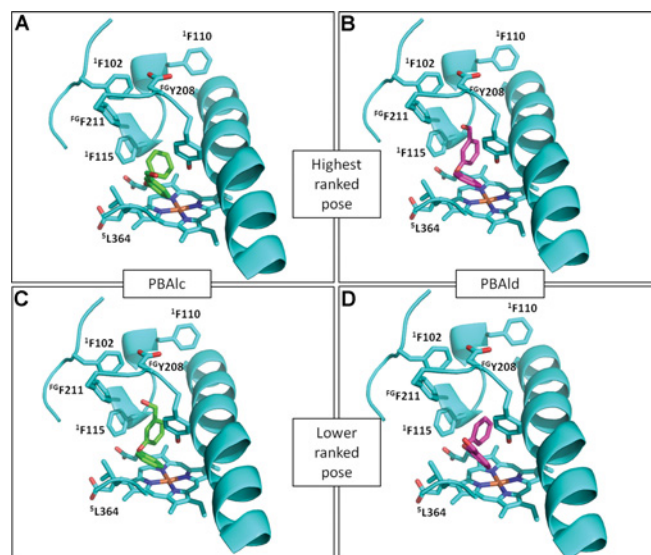


Figure 3 Predicted binding modes of PBAIc and PBAId in the CYP6Z8 model

PBAIc (green) and PBAId (purple) binding are shown for the highest-ranked poses (A and B) and lower-ranked poses (C and D). Residues that project into the active site are labelled. Superscript text refers to amino acids belonging to SRS1 (¹), FG loop (^{FG}) and SRS5 (⁵) regions.

In vivo assays and regulation of CYP6Z8 expression by pyrethroid metabolites

Incubating alive *Ae. aegypti* third instar larvae with PBAIc for 24 h revealed a concomitant decrease in PBAIc in the growing medium and an increase in PBA together with other minor metabolites, suggesting that the PBA produced is directly excreted by larvae without further modification (Figure 5).

In order to assess whether CYP6Z8 transcription is regulated by its substrates and/or products, larvae were exposed for 24 h to various concentrations of PBAIc, PBAId and PBA. The transcription levels of CYP6Z8 compared with unexposed larvae were then compared using qPCR (Supplementary Figure S4 at <http://www.biochemj.org/bj/455/bj4550075add.htm>). CYP6Z8 transcription was significantly induced by all compounds (2.0–3.4-fold) with a moderate dose-dependent effect.

DISCUSSION

The present study aimed at co-expressing *Ae. aegypti* CYP6Z8 and AeCPR in a heterologous system, characterizing its activity towards known P450 substrates and investigating its role in the metabolism of insecticides.

CYP6Z8 sequence analysis revealed several variations in the Bora-Bora strain compared with the genome sequence (Liverpool strain, VectorBase AegL1.2 gense). In total 49 nucleotide variations, including 13 variations leading to amino acid changes, were found, confirming the high polymorphism of mosquito CYPs. These non-synonymous variations did not occur in the conserved P450 signature motifs [12]. Only one amino acid change occurred in an SRS at a position not strictly conserved among CYP6Zs. As confirmed by 3D modelling, this replacement (F285L) occurring in the oxygen-binding motif (SRS4) is likely not to affect CYP6Z8 substrate specificity, as physicochemical properties of these two amino acids are similar (Figure 4).

The yeast P450 expression system developed by Pompon et al. [32] was chosen to create a novel genetically modified yeast strain allowing the co-expression of any mosquito P450 together with

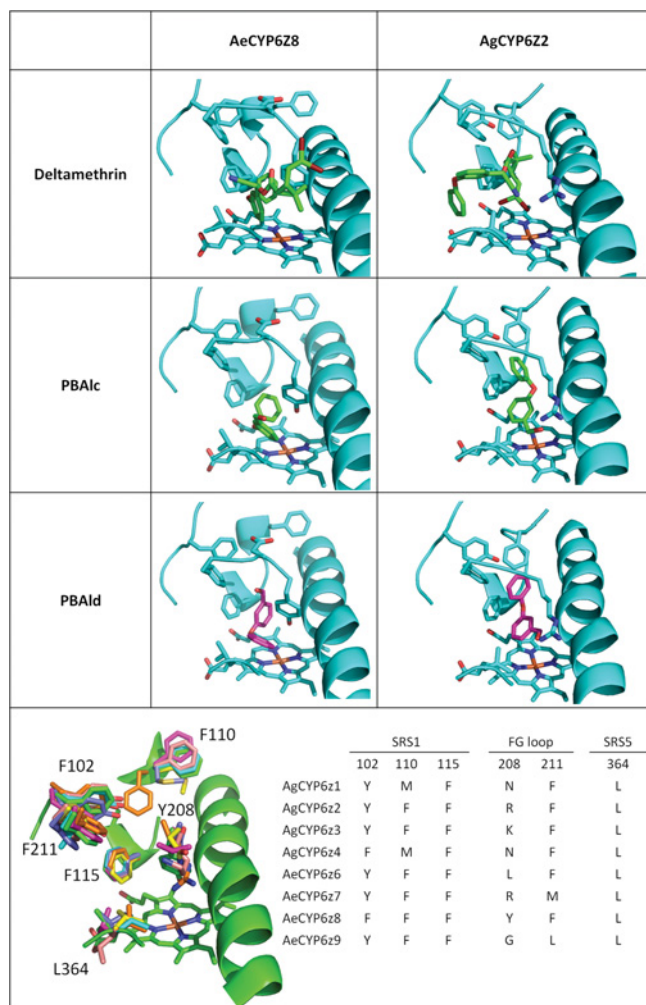


Figure 4 Molecular models of CYP6Zs

Top panel: comparison of deltamethrin, PBAIc and PBAId docking in AeCYP6Z8 and AgCYP6Z2 (highest-ranked poses). Bottom panel: alignment of AeCYP6Z8 (green), AeCYP6Z9 (blue), AeCYP6Z6 (purple), AgCYP6Z4 (yellow), AgCYP6Z3 (pink), AgCYP6Z1 (dark blue) and AgCYP6Z2 (orange). The table shows a comparison of residues projecting into the active site. Residues are labelled according to the position on CYP6Z8. Ae, *Ae. aegypti*; Ag, *An. gambiae*.

its CPR. Such a system has been successfully used to express and characterize various P450s from human, plants and fungi [32,40–42]. The results of the present study show that replacing yeast CPR by mosquito CPR under a galactose-inducible promoter enables the W(AeR) strain to overexpress mosquito CPR at a high level. Transforming the W(AeR) strain with an expression plasmid carrying the *CYP6Z8* gene under the same promoter allowed us to produce a functional mosquito CPR–P450 membrane system. As CPR is highly conserved in mosquitoes, this new tool should allow the functional expression of any microsomal mosquito P450. This was recently confirmed by the successful expression of functional *An. gambiae* P450s using the W(AeR) yeast strain (A. Chandor-Proust, M. Paine and J.-P. David, unpublished work). To our knowledge, this is the first time a mosquito P450 has been successfully expressed in yeast, along with its redox partner and without protein sequence modification. Although *E. coli* is commonly used to express P450s and has higher yields, some eukaryote P450s are intractable for expression. The yeast system thereby provides a useful alternative method with the advantage

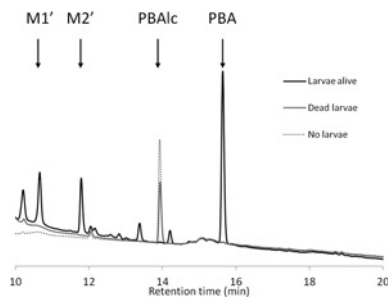


Figure 5 *In vivo* metabolism of PBAIc

HPLC chromatograms showing excreted metabolites after exposing *Ae. aegypti* larvae alive or dead for 24 h to 2 mg/l PBAIc. PBAIc and main metabolites are indicated by arrows.

of having eukaryotic cellular and redox machinery plus organelle structure appropriate for the translation of eukaryotic P450s.

The results of the present study clearly indicate that our recombinant CYP6Z8 is functional and able to metabolize various standard P450 substrates. Kinetic data suggest that benzyloxresorufin is preferred, followed by ethoxyresorufin. Supplementing reactions with purified *Ae. aegypti* Cyt b5 did not affect CYP6Z8 substrate specificity and activity. Whether CYP6Z8 does not strongly interact with Cyt b5 or the co-expression of AeCPR and CYP6Z8 produces such a high P450/CPR ratio making the presence of an extra electron donor, such as Cyt b5, not necessary requires further investigation [43].

Then, the ability of CYP6Z8 to metabolize various xenobiotics, including insecticides, was investigated. As for *An. gambiae* CYP6Z2, CYP6Z8 did not metabolize permethrin and deltamethrin [23,24]. In contrast with CYP6Z1, CYP6Z8 was not capable of metabolizing DDT either. However, CYP6Z8 metabolized α -naphthoflavone and the stilbene resveratrol, as did CYP6Z2 [24].

In mammals it has been demonstrated that pyrethroids can be hydrolysed by carboxylesterases leading to the production of PBAIc and PBAId and that these metabolites can be further processed by P450s into PBA [44–46]. Recently, *in vitro* metabolism assays with microsomes extracted from *Ae. aegypti* larvae suggested that this detoxification pathway occurs in mosquitoes [47]. Because CYP6Zs are frequently overtranscribed in mosquito populations resistant and/or exposed to pyrethroids, the ability of CYP6Z8 to metabolize common pyrethroid metabolites was investigated further. Our results clearly demonstrate that CYP6Z8 is capable of metabolizing PBAIc into PBA, with PBAId being a transitory metabolite (Figure 6). Similarly, we showed that its *An. gambiae* orthologue CYP6Z2 can also metabolize PBAIc in the same manner, supporting the functional orthology of these two mosquito P450s. To our knowledge, CYP6Z8 and CYP6Z2 are the first insect P450s shown to metabolize pyrethroid metabolites generated by carboxylesterase hydrolysis.

Two minor more hydrophilic metabolites (M1 and M2) were also detected. Examination of M1 and M2 metabolites by LC–MS and MS/MS did not allow the absolute identification of their chemical structure. The behaviour of PBAIc in positive-mode electrospray was not trivial as the parental ions (183 *m/z*) did not correspond to the theoretical mass (201 *m/z*), but suggested its dehydration. Despite this, no direct additions of alcohol function (+16 *m/z*) were observed for M1 and M2, suggesting that these compounds are not simply hydroxylated. Previous studies have shown that the direct attack of pyrethroids by P450s often produces 4'-hydroxylation in insects [17,48]. The results of the

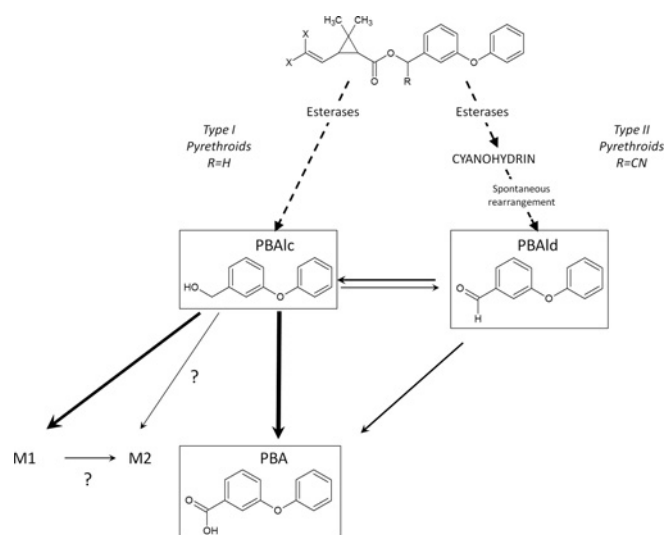


Figure 6 Proposed role of CYP6Z8 in pyrethroid metabolism

Broken arrows indicates a first attack by carboxylesterases [52]. Solid arrows indicate CYP6Z8 NADPH-dependent transformations. Arrow width is proportional to the initial reaction rate of metabolite production. Hypothetical reactions forming the M2 metabolite are indicated by question marks. In the generic representation of pyrethroids, X represents a halogenated substituent and R is either a H (type I pyrethroid) or CN (type II pyrethroid) group.

present study suggest that the attack of pyrethroid metabolites generated by esterase hydrolysis by CYP6Zs is different.

Because PBA is not metabolized by CYP6Z8, M1 and M2 can only represent metabolites of PBAIc or PBAId. Common fragmentation ions were found between M1 and PBAIc, suggesting a similar backbone. In addition, M1 and M2 HPLC R_t were not affected by pH variations as opposed to PBAId and PBA, confirming that they do not carry acid or aldehyde functions. Overall, these results support the hypothesis of M1 originating from PBAIc and M2 being a secondary metabolite of M1 (Figure 6). Finally, *in vivo* experiments revealed that PBA is the major metabolite produced and is excreted from mosquitoes without further modification. In contrast, M1 and M2 metabolites were not excreted from mosquitoes. Instead, two more polar metabolites (M1' and M2' in Figure 5) separated by a comparable ΔR_t were observed, suggesting that M1 and M2 are further processed before being excreted.

In silico 3D modelling of CYP6Z–substrate interactions confirmed our experimental findings on CYP6Z8 and CYP6Z2 with good binding scores and limited clashes of pyrethroid metabolites in the active site. Comparing 3D models between various *Aedes* and *Anopheles* CYP6Zs supports the capacity of other mosquito CYP6Zs to metabolize these and produce similar metabolites (Figure 4). The inability of CYP6Z8 and CYP6Z2 to metabolize deltamethrin was supported by 3D models showing good binding scores but high clashes between active-site residues and substrate or within substrate itself. Bulky residues in the FG loop and SRS1 and SRS5 of mosquito CYP6Zs are probably preventing the metabolism of large pyrethroids. Indeed, while known pyrethroid metabolizers such as CYP6M2, CYP6B8 and CYP3A1 may require aromatic residues in the active site at position Phe¹¹⁵ to π -stack with the phenyl ring, and/or Phe¹⁰² to bind with the benzyl ring [17,49,50], the extensive network of aromatic residues in the CYP6Z subfamily may restrict the binding of the large pyrethroids, but stabilize the binding of smaller compounds such as PBAIc or PBAId.

Overall, the results of the present study lift the veil on the pivotal role of CYP6Z8 and CYP6Z2 in pyrethroid biodegradation in mosquitoes and clarify why they have frequently been associated with resistance [15,21,22,29,51], whereas their capacity to metabolize pyrethroid insecticides could not be validated [23,24]. This is the first direct evidence that secondary metabolism of insecticide pyrethroids by P450s is linked to resistance. Our results strongly support the role of these P450s following the action of carboxylesterases in order to clear mosquito body from these metabolites. Although hydrolysed pyrethroid metabolites such as PBAIc and PBAId are far less toxic than intact pyrethroids, their accumulation is likely to be detrimental to mosquitoes. Therefore the role of CYP6Zs in the mosquito response to pyrethroids is not negligible and the over-transcription of these genes in natural populations should be considered as supporting evidence of metabolic resistance.

Genes encoding carboxylesterases have been frequently found to be overtranscribed in pyrethroid-resistant populations and their role in pyrethroid biodegradation has been established *in vitro* [47]. However, to our knowledge, no particular mosquito carboxylesterase has yet been validated as a pyrethroid metabolizer. A better understanding of insecticide degradation pathways in mosquitoes will allow for the pinpointing of action points to develop new strategies to overcome resistance mechanisms. In this frame, estimating the relative importance of mosquito detoxification enzymes in resistance is also important, but not trivial. Any enzyme involved in the insecticide degradation pathway may have a different importance in the resistant phenotype depending on its expression profile, the step catalysed, its substrate specificity and turnover rate, and the toxicity and lipophilicity of the metabolites produced. This certainly represents the next research challenge for understanding how mosquitoes adjust their metabolism to resist insecticides and better manage these resistance mechanisms.

AUTHOR CONTRIBUTION

Alexia Chandor-Proust contributed to conceiving the study, performed experiments, analysed results and wrote the paper. Jaclyn Bibby and Mark Paine performed the structural modelling work and helped draft the paper. Myriam Régent-Kloekner performed qPCR experiments and contributed to *in vivo* experiments. Jessica Roux contributed to protein expression work. Emilie Guittard-Crilat performed CYP6Z8 cloning. Rodolphe Poupardin and Muhammad Asam Riaz helped conceive the study. Chantal Dauphin-Villemant contributed to cloning and *in vitro* experiments and helped draft the paper. Stéphane Reynaud contributed to the study design, data analysis and helped write the paper. Jean-Philippe David conceived and co-ordinated the study, analysed results and wrote the paper. All authors read and approved the final paper.

ACKNOWLEDGEMENTS

We thank T. Gaude and S. Veyrenc for technical assistance with mosquito rearing and insectary maintenance. We thank Dr P. Urban for useful comments on the paper, and Dr Y. Gimbert and L. Fort for their help in analysing MS data.

FUNDING

This work and A.C.-P. were supported by the French National Research Agency Project [ANR project number 07SEST14 MOSQUITO-ENV]. A.C.-P. was also funded by a Grenoble University Research Fellowship. The Grenoble Mass Spectrometry facility (PSM/ICMG) used in the present study was funded by the French NanoSciences Foundation, the Rhone-Alpes Region, the CNRS and Grenoble University. We also acknowledge additional funding from the EU Seventh Framework programme [grant number 265660 AvecNet].

REFERENCES

- 1 World Health Organization (2010) Working to overcome the global impact of neglected tropical diseases: first WHO report on neglected tropical diseases, ISBN 978 92 4 1564090
- 2 Hemingway, J., Beaty, B. J., Rowland, M., Scott, T. W. and Sharp, B. L. (2006) The Innovative Vector Control Consortium: improved control of mosquito-borne diseases. *Trends Parasitol.* **22**, 308–312
- 3 Killeen, G. F., Fillinger, U. and Knols, B. G. (2002) Advantages of larval control for African malaria vectors: low mobility and behavioural responsiveness of immature mosquito stages allow high effective coverage. *Malar. J.* **1**, 8
- 4 Hemingway, J. and Ranson, H. (2000) Insecticide resistance in insect vectors of human disease. *Annu. Rev. Entomol.* **45**, 371–391
- 5 David, J. P., Mahmoud Ismail, H., Chandor-Proust, A. and Paine, M. J. I. (2013) Role of cytochrome P450s in insecticide resistance: impact on the control of mosquito-borne diseases and use of insecticides on earth. *Philos. Trans. R. Soc. London Ser. B* **368**, 20120429
- 6 Nkya, T. E., Akhouayri, I., Kisinza, W. and David, J. P. (2012) Impact of environment on mosquito response to pyrethroid insecticides: facts, evidences and prospects. *Insect Biochem. Mol. Biol.* **43**, 407–416
- 7 Li, X., Schuler, M. A. and Berenbaum, M. R. (2007) Molecular mechanisms of metabolic resistance to synthetic and natural xenobiotics. *Annu. Rev. Entomol.* **52**, 231–253
- 8 Scott, J. G. (1999) Cytochromes P450 and insecticide resistance. *Insect Biochem. Mol. Biol.* **29**, 757–777
- 9 Feyereisen, R. (2011) Arthropod CYPomes illustrate the tempo and mode in P450 evolution. *Biochim. Biophys. Acta* **1814**, 19–28
- 10 Murataliev, M. B., Guzov, V. M., Walker, F. A. and Feyereisen, R. (2008) P450 reductase and cytochrome b5 interactions with cytochrome P450: effects on house fly CYP6A1 catalysis. *Insect Biochem. Mol. Biol.* **38**, 1008–1015
- 11 Jousen, N., Heckel, D. G., Haas, M., Schuphan, I. and Schmidt, B. (2008) Metabolism of imidacloprid and DDT by P450 CYP6G1 expressed in cell cultures of *Nicotiana tabacum* suggests detoxification of these insecticides in Cyp6g1-overexpressing strains of *Drosophila melanogaster*, leading to resistance. *Pest Manage. Sci.* **64**, 65–73
- 12 Karunker, I., Morou, E., Nikou, D., Nauen, R., Sertchook, R., Stevenson, B. J., Paine, M. J., Morin, S. and Vontas, J. (2009) Structural model and functional characterization of the *Bemisia tabaci* CYP6CM1vQ, a cytochrome P450 associated with high levels of imidacloprid resistance. *Insect Biochem. Mol. Biol.* **39**, 697–706
- 13 Ranson, H., Claudianos, C., Ortell, F., Abgrall, C., Hemingway, J., Sharakhova, M. V., Unger, M. F., Collins, F. H. and Feyereisen, R. (2002) Evolution of supergene families associated with insecticide resistance. *Science* **298**, 179–181
- 14 Strode, C., Wondji, C. S., David, J. P., Hawkes, N. J., Lumjuan, N., Nelson, D. R., Drane, D. R., Karunaratne, S. H., Hemingway, J., Black, 4th, W. C. and Ranson, H. (2008) Genomic analysis of detoxification genes in the mosquito *Aedes aegypti*. *Insect Biochem. Mol. Biol.* **38**, 113–123
- 15 David, J. P., Strode, C., Vontas, J., Nikou, D., Vaughan, A., Pignatelli, P. M., Louis, C., Hemingway, J. and Ranson, H. (2005) The *Anopheles gambiae* detoxification chip: a highly specific microarray to study metabolic-based insecticide resistance in malaria vectors. *Proc. Natl. Acad. Sci. U.S.A.* **102**, 4080–4084
- 16 Muller, P., Warr, E., Stevenson, B. J., Pignatelli, P. M., Morgan, J. C., Steven, A., Yawson, A. E., Mitchell, S. N., Ranson, H., Hemingway, J. et al. (2008) Field-caught permethrin-resistant *Anopheles gambiae* overexpress CYP6P3, a P450 that metabolises pyrethroids. *PLoS Genet.* **4**, e1000286
- 17 Stevenson, B. J., Bibby, J., Pignatelli, P., Muangnoicharoen, S., O'Neill, P. M., Lian, L. Y., Muller, P., Nikou, D., Steven, A., Hemingway, J. et al. (2011) Cytochrome P450 6M2 from the malaria vector *Anopheles gambiae* metabolizes pyrethroids: sequential metabolism of deltamethrin revealed. *Insect Biochem. Mol. Biol.* **41**, 492–502
- 18 Riveron, J. M., Irving, H., Ndula, M., Barnes, K. G., Ibrahim, S. S., Paine, M. J. and Wondji, C. S. (2013) Directionally selected cytochrome P450 alleles are driving the spread of pyrethroid resistance in the major malaria vector *Anopheles funestus*. *Proc. Natl. Acad. Sci. U.S.A.* **110**, 252–257
- 19 Stevenson, B. J., Pignatelli, P., Nikou, D. and Paine, M. J. (2012) Pinpointing P450s associated with pyrethroid metabolism in the dengue vector, *Aedes aegypti*: developing new tools to combat insecticide resistance. *PLoS Negl. Trop. Dis.* **6**, e1595
- 20 Marcombe, S., Poupardin, R., Darriet, F., Reynaud, S., Bonnet, J., Strode, C., Brengues, C., Yebakima, A., Ranson, H., Corbel, V. and David, J. P. (2009) Exploring the molecular basis of insecticide resistance in the dengue vector *Aedes aegypti*: a case study in Martinique Island (French West Indies). *BMC Genomics* **10**, 494
- 21 Nikou, D., Ranson, H. and Hemingway, J. (2003) An adult-specific CYP6 P450 gene is overexpressed in a pyrethroid-resistant strain of the malaria vector, *Anopheles gambiae*. *Gene* **318**, 91–102
- 22 Poupardin, R., Riaz, M. A., Jones, C. M., Chandor-Proust, A., Reynaud, S. and David, J. P. (2012) Do pollutants affect insecticide-driven gene selection in mosquitoes? Experimental evidence from transcriptomics. *Aquat. Toxicol.* **114–115**, 49–57
- 23 Chiu, T. L., Wen, Z., Rupasinghe, S. G. and Schuler, M. A. (2008) Comparative molecular modeling of *Anopheles gambiae* CYP6Z1, a mosquito P450 capable of metabolizing DDT. *Proc. Natl. Acad. Sci. U.S.A.* **105**, 8855–8860
- 24 McLaughlin, L. A., Niaz, U., Bibby, J., David, J. P., Vontas, J., Hemingway, J., Ranson, H., Sutcliffe, M. J. and Paine, M. J. (2008) Characterization of inhibitors and substrates of *Anopheles gambiae* CYP6Z2. *Insect Mol. Biol.* **17**, 125–135
- 25 David, J. P., Coissac, E., Melodelima, C., Poupardin, R., Riaz, M. A., Chandor-Proust, A. and Reynaud, S. (2010) Transcriptome response to pollutants and insecticides in the dengue vector *Aedes aegypti* using next-generation sequencing technology. *BMC Genomics* **11**, 216
- 26 Poupardin, R., Reynaud, S., Strode, C., Ranson, H., Vontas, J. and David, J. P. (2008) Cross-induction of detoxification genes by environmental xenobiotics and insecticides in the mosquito *Aedes aegypti*: impact on larval tolerance to chemical insecticides. *Insect Biochem. Mol. Biol.* **38**, 540–551
- 27 Poupardin, R., Riaz, M. A., Vontas, J., David, J. P. and Reynaud, S. (2010) Transcription profiling of eleven cytochrome P450s potentially involved in xenobiotic metabolism in the mosquito *Aedes aegypti*. *Insect Mol. Biol.* **19**, 185–193
- 28 Riaz, M. A., Poupardin, R., Reynaud, S., Strode, C., Ranson, H. and David, J. P. (2009) Impact of glyphosate and benzoflajpyrene on the tolerance of mosquito larvae to chemical insecticides. Role of detoxification genes in response to xenobiotics. *Aquat. Toxicol.* **93**, 61–69
- 29 Marcombe, S., Mathieu, R. B., Pocquet, N., Riaz, M. A., Poupardin, R., Selior, S., Darriet, F., Reynaud, S., Yebakima, A., Corbel, V. et al. (2012) Insecticide resistance in the dengue vector *Aedes aegypti* from Martinique: distribution, mechanisms and relations with environmental factors. *PLoS ONE* **7**, e30989
- 30 Guzov, V. M., Houston, H. L., Murataliev, M. B., Walker, F. A. and Feyereisen, R. (1996) Molecular cloning, overexpression in *Escherichia coli*, structural and functional characterization of house fly cytochrome b5. *J. Biol. Chem.* **271**, 26637–26645
- 31 Holmans, P. L., Shet, M. S., Martin-Wixtrom, C. A., Fisher, C. W. and Estabrook, R. W. (1994) The high-level expression in *Escherichia coli* of the membrane-bound form of human and rat cytochrome b5 and studies on their mechanism of function. *Arch. Biochem. Biophys.* **312**, 554–565
- 32 Pompon, D., Louerat, B., Brönne, A. and Urban, P. (1996) Yeast expression of animal and plant P450s in optimized redox environments. *Methods Enzymol.* **272**, 51–64
- 33 Gietz, R. D. and Schiestl, R. H. (2007) High-efficiency yeast transformation using the LiAc/SS carrier DNA/PEG method. *Nat. Protoc.* **2**, 31–34
- 34 Bradford, M. M. (1976) A rapid and sensitive method for the quantitation of microgram quantities of protein utilizing the principle of protein-dye binding. *Anal. Biochem.* **72**, 248–254
- 35 Omura, T. and Sato, R. (1964) The carbon monoxide-binding pigment of liver microsomes. I. Evidence for its hemoprotein nature. *J. Biol. Chem.* **239**, 2370–2378
- 36 Black, S. D. and Coon, M. J. (1982) Structural features of liver microsomal NADPH-cytochrome P-450 reductase. Hydrophobic domain, hydrophilic domain, and connecting region. *J. Biol. Chem.* **257**, 5929–5938
- 37 Pfaffl, M. W. (2001) A new mathematical model for relative quantification in real-time RT-PCR. *Nucleic Acids Res.* **29**, 6
- 38 Yano, J. K., Wester, M. R., Schoch, G. A., Griffin, K. J., Stout, C. D. and Johnson, E. F. (2004) The structure of human microsomal cytochrome P450 3A4 determined by X-ray crystallography to 2.05-Å resolution. *J. Biol. Chem.* **279**, 38091–38094
- 39 Verdonk, M. L., Cole, J. C., Hartshorn, M. J., Murray, C. W. and Taylor, R. D. (2003) Improved protein-ligand docking using GOLD. *Proteins* **52**, 609–623
- 40 Chung, W. G., Sen, A., Wang-Buhler, J. L., Yang, Y. H., Lopez, N., Merrill, G. F., Miranda, C. L., Hu, C. H. and Buhler, D. R. (2004) cDNA-directed expression of a functional zebrafish CYP1A in yeast. *Aquat. Toxicol.* **70**, 111–121
- 41 Bozak, K. R., O'Keefe, D. P. and Christoffersen, R. E. (1992) Expression of a ripening-related avocado (*Persea americana*) cytochrome P450 in yeast. *Plant Physiol.* **100**, 1976–1981
- 42 Urban, P., Werck-Reichhart, D., Teutsch, H. G., Durst, F., Regnier, S., Kazmaier, M. and Pompon, D. (1994) Characterization of recombinant plant cinnamate 4-hydroxylase produced in yeast. Kinetic and spectral properties of the major plant P450 of the phenylpropanoid pathway. *Eur. J. Biochem.* **222**, 843–850
- 43 Schenkman, J. B. and Jansson, I. (2003) The many roles of cytochrome b5. *Pharmacol. Ther.* **97**, 139–152
- 44 Godin, S. J., Scollon, E. J., Hughes, M. F., Potter, P. M., DeVito, M. J. and Ross, M. K. (2006) Species differences in the *in vitro* metabolism of deltamethrin and estenvalerate: differential oxidative and hydrolytic metabolism by humans and rats. *Drug Metab. Dispos.* **34**, 1764–1771

- 45 Nakamura, Y., Sugihara, K., Sone, T., Isobe, M., Ohta, S. and Kitamura, S. (2007) The *in vitro* metabolism of a pyrethroid insecticide, permethrin, and its hydrolysis products in rats. *Toxicology* **235**, 176–184
- 46 Takaku, T., Mikata, K., Matsui, M., Nishioka, K., Isobe, N. and Kaneko, H. (2011) *In vitro* metabolism of trans-permethrin and its major metabolites, PBalc and PBacid, in humans. *J. Agric. Food Chem.* **59**, 5001–5005
- 47 Somwang, P., Yanola, J., Suwan, W., Walton, C., Lumjuan, N., Prapanthadara, L. A. and Somboon, P. (2011) Enzymes-based resistant mechanism in pyrethroid resistant and susceptible *Aedes aegypti* strains from northern Thailand. *Parasitol. Res.* **109**, 531–537
- 48 Khambay, B. and Jewess, P. (2004) Pyrethroids. In *Comprehensive Molecular Insect Science* (Gilbert, L. I., Iatrou, K. and Gill, S. S., eds), section 6.1, pp. 1–29, Elsevier, Oxford
- 49 Li, X., Baudry, J., Berenbaum, M. R. and Schuler, M. A. (2004) Structural and functional divergence of insect CYP6B proteins: from specialist to generalist cytochrome P450. *Proc. Natl. Acad. Sci. U.S.A.* **101**, 2939–2944
- 50 Scollon, E. J., Starr, J. M., Godin, S. J., DeVito, M. J. and Hughes, M. F. (2009) *In vitro* metabolism of pyrethroid pesticides by rat and human hepatic microsomes and cytochrome p450 isoforms. *Drug Metab. Dispos.* **37**, 221–228
- 51 Muller, P., Donnelly, M. J. and Ranson, H. (2007) Transcription profiling of a recently colonised pyrethroid resistant *Anopheles gambiae* strain from Ghana. *BMC Genomics* **8**, 36
- 52 Laffin, B., Chavez, M. and Pine, M. (2010) The pyrethroid metabolites 3-phenoxybenzoic acid and 3-phenoxybenzyl alcohol do not exhibit estrogenic activity in the MCF-7 human breast carcinoma cell line or Sprague–Dawley rats. *Toxicology* **267**, 39–44

Received 25 April 2013/10 July 2013; accepted 11 July 2013

Published as BJ Immediate Publication 11 July 2013, doi:10.1042/BJ20130577

SUPPLEMENTARY ONLINE DATA

The central role of mosquito cytochrome P450 CYP6Zs in insecticide detoxification revealed by functional expression and structural modelling

Alexia CHANDOR-PROUST*, Jaclyn BIBBY†, Myriam RÉGENT-KLOECKNER*, Jessica ROUX*, Emilie GUITTARD-CRILAT‡, Rodolphe POUPARDIN*§, Muhammad Asam RIAZ*||, Mark PAINE§, Chantal DAUPHIN-VILLEMANT‡¶, Stéphane REYNAUD* and Jean-Philippe DAVID*1

*Laboratoire d'Ecologie Alpine (LECA), UMR 5553 CNRS, Université de Grenoble, Grenoble 38041, France, †Institute of Integrative Biology, University of Liverpool, Liverpool L69 7ZB, U.K., ‡Université Pierre et Marie Curie, CNRS, Paris 75005, France, §Liverpool School of Tropical Medicine, Liverpool L3 5QA, U.K., ||Department of Agri-Entomology, University College of Agriculture, University of Sargodha, Sargodha, Pakistan, and ¶Department of Ecology and Evolution, University of Lausanne, Lausanne 1015, Switzerland

```

CYP6Z8_Bora ATGTTTCATCTACACCTTCGCACCTCTCTGGTTGGCAGTGGGTTGGCCATCCGCTACATC 60
CYP6Z8_Liv ATGTTTCATCTACACCTTCGCACCTCTCTGGTTGGCAGTGGGTTGGCCATCCGCTACATC
CYP6Z8_Bora TACTCGTATGGGATCGGAATGGATTGCGGAGCATCAAACCGCACATCCCTTACGGCAAC 120
CYP6Z8_Liv TACTCGTACTGGGATCGGAATGGATTGCGGAGCATCAAACCGCACATCCCTTACGGCAAC
CYP6Z8_Bora CTGAAAACCGTGCCCAACGAGCAGGAATCTTCCGGAGTGCACATGTGACCTCTACTGG 180
CYP6Z8_Liv CTGAAAACCGTGCCCAACGAGCAGGAATCTTCCGGAGTGCACATGTGACCTCTACTGG
CYP6Z8_Bora AAGTCCAAGATCGACTGTGGGAATCTATCTGTTCTTCCGGCCGGCTGTCTGATTGGA 240
CYP6Z8_Liv AAGTCCAAGATCGACTGTGGGAATCTATCTGTTCTTCCGGCCGGCTGTCTGATTGGA
CYP6Z8_Bora GATGCGCACTTAGCACAGCAAAATGATGACGACGACTTCCAGCCATTTCCAGACCGTGGC 300
CYP6Z8_Liv GATGCGCACTTAGCACAGCAAAATGATGACGACGACTTCCAGCCATTTCCAGACCGTGGC
CYP6Z8_Bora GTCTTTGCAACGAAGAAGTGCATCCTTCTCTGGGAATCTGTTGCGCTTCTGCTGGGAAG 360
CYP6Z8_Liv GTCTTTGCAACGAAGAAGTGCATCCTTCTCTGGGAATCTGTTGCGCTTCTGCTGGGAAG
CYP6Z8_Bora CGTTGGCCCAATCTGAGGAAACAAGTTTACCACCTGTTCCACCCGGCAACTTCGCTGC 420
CYP6Z8_Liv CGTTGGCCCAATCTGAGGAAACAAGTTTACCACCTGTTCCACCCGGCAACTTCGCTGC
CYP6Z8_Bora ATGATGCCAATCTTAAGCGTTGGACACAAGTGCAGAAATGCTCCGAGCCAGCTGCC 480
CYP6Z8_Liv ATGATGCCAATCTTAAGCGTTGGACACAAGTGCAGAAATGCTCCGAGCCAGCTGCC
CYP6Z8_Bora AAAAAACAGGAAGTGTGGAAATTCGGGAATTTGGTGTACAGATGTGTGGACATAAAT 540
CYP6Z8_Liv AAAAAACAGGAAGTGTGGAAATTCGGGAATTTGGTGTACAGATGTGTGGACATAAAT
CYP6Z8_Bora GCTTCGGTATTTTTCGGTTTCGAAGCAAACTGATTAATGATCCGAAACGATGGCTCATC 600
CYP6Z8_Liv GCTTCGGTATTTTTCGGTTTCGAAGCAAACTGATTAATGATCCGAAACGATGGCTCATC
CYP6Z8_Bora CAAAATCTCGCCGAACCTCAGTATGACGAGTTTTTAAACAATCTCCGGCTGCTGCATCG 660
CYP6Z8_Liv CAAAATCTCGCCGAACCTCAGTATGACGAGTTTTTAAACAATCTCCGGCTGCTGCATCG
CYP6Z8_Bora TTTATCTGCTGAATTTGAAGTTAAAGCGAATTTCAATCGTTGAGCCCTGAGATGATC 720
CYP6Z8_Liv TTTATCTGCTGAATTTGAAGTTAAAGCGAATTTCAATCGTTGAGCCCTGAGATGATC
CYP6Z8_Bora CGATTGTAACGACATTTGTAACGAAACGATTTGAGCACCCTGAAAAGCAAAATGATACC 780
CYP6Z8_Liv CGATTGTAACGACATTTGTAACGAAACGATTTGAGCACCCTGAAAAGCAAAATGATACC
CYP6Z8_Bora GAAAAGATTTCAATCAACTGCTATCGATCTTCCGAGAGGATCCCAACAACGAGAA 840
CYP6Z8_Liv GAAAAGATTTCAATCAACTGCTATCGATCTTCCGAGAGGATCCCAACAACGAGAA
CYP6Z8_Bora GCAACTTTGGTTTGAAGAGTGCAGCAAAAGTATTCTGTTTATGATAGCTGGTTCG 900
CYP6Z8_Liv GCAACTTTGGTTTGAAGAGTGCAGCAAAAGTATTCTGTTTATGATAGCTGGTTCG
CYP6Z8_Bora GACACATCCCAAGTGGCGTGCATCTCACACTGCACGAGCTGACCCAAAATGGGAAACC 960
CYP6Z8_Liv GACACATCCCAAGTGGCGTGCATCTCACACTGCACGAGCTGACCCAAAATGGGAAACC
CYP6Z8_Bora ATGGAAAACACAGCAGGAAATCGATGAAATGTTGTTGAAAACAGCGGTAACCTACT 1020
CYP6Z8_Liv ATGGAAAACACAGCAGGAAATCGATGAAATGTTGTTGAAAACAGCGGTAACCTACT
CYP6Z8_Bora TATGATGAAATTAAGAGATGCTCACTACCTAGACTTGTGTCAAGAAACCCCTCGAAG 1080
CYP6Z8_Liv TATGATGAAATTAAGAGATGCTCACTACCTAGACTTGTGTCAAGAAACCCCTCGAAG
CYP6Z8_Bora TATCCAGGCTCGCAATTTGAATCGTGAATGCAACAAAAGTATGCTGTTCCAACTCG 1140
CYP6Z8_Liv TATCCAGGCTCGCAATTTGAATCGTGAATGCAACAAAAGTATGCTGTTCCAACTCG
CYP6Z8_Bora AACATCTACTCAAGAAGGAACTCAGTGTGTGATCCCATGCTGGCGTACGGTATGGAT 1200
CYP6Z8_Liv AACATCTACTCAAGAAGGAACTCAGTGTGTGATCCCATGCTGGCGTACGGTATGGAT
CYP6Z8_Bora GAAAAATATTTCCAGAACCCGAAATCGATATCTCCGAGAGGTTGCACAAACTACGAAA 1260
CYP6Z8_Liv GAAAAATATTTCCAGAACCCGAAATCGATATCTCCGAGAGGTTGCACAAACTACGAAA
CYP6Z8_Bora AACTACGACGAAAAGGCACTCTATCCATTCCGAGAAAGTCTCGGAATTTGATAGCTTTC 1320
CYP6Z8_Liv AACTACGACGAAAAGGCACTCTATCCATTCCGAGAAAGTCTCGGAATTTGATAGCTTTC
CYP6Z8_Bora AGAATGGGCGTAATGTTTCCAAGATTTGTTGGTTTGGCTTCTGTCOGGATCAACTTT 1380
CYP6Z8_Liv AGAATGGGCGTAATGTTTCCAAGATTTGTTGGTTTGGCTTCTGTCOGGATCAACTTT
CYP6Z8_Bora GAAGCCACCCGAGGTCGAAAATCACTCACTCCTTCAACAGTGGCCCTGTAACCAAG 1440
CYP6Z8_Liv GAAGCCACCCGAGGTCGAAAATCACTCACTCCTTCAACAGTGGCCCTGTAACCAAG
CYP6Z8_Bora GGGCCATTCGGTGAAGATATCGATTCCGCTGA 1473
CYP6Z8_Liv GGGCCATTCGGTGAAGATATCGATTCCGCTGA
    
```

Figure S1 Alignment of cloned CYP6Z8 cDNA compared with the genome sequence

Coding sequence cloned from Bora-Bora strain cDNA was compared with the cDNA sequence extracted from VectorBase (AaeGL1.2 geneset, Liverpool strain). Differences are shaded.

```

CYP6Z8_Bora MFIYTFALFWLAVAFIRVYISYNDKNGLSIKPHIPIYGNLKWNRMTESFGVATCDLHW 60
CYP6Z8_Liv MFIYTFALFWLAVAFIRVYISYNDKNGLSIKPHIPIYGNLKWNRMTESFGVATCDLHW
CYP6Z8_Bora KSKDRLVGIYLFRRFAVLIRDHAHQIMTDFSHFDKRGVFCNEEVDFPSANLFLAGK 120
CYP6Z8_Liv KSKDRLVGIYLFRRFAVLIRDHAHQIMTDFSHFDKRGVFCNEEVDFPSANLFLAGK
CYP6Z8_Bora FNNRNLNKKFTPLFTGGQLRCMPFIILVGHKLQNVLEPAAKKQVELEIRELVSRCLDII 180
CYP6Z8_Liv FNNRNLNKKFTPLFTGGQLRCMPFIILVGHKLQNVLEPAAKKQVELEIRELVSRCLDII
CYP6Z8_Bora ASVFFGFEANCINDPDAFIQNLREIYDGFNNLRAAAFFICPELLKLRSSLSPEM 240
CYP6Z8_Liv ASVFFGFEANCINDPDAFIQNLREIYDGFNNLRAAAFFICPELLKLRSSLSPEM
CYP6Z8_Bora RFVTDIVTKQIEHREKNNVTRKDFQLLIDLRREDNNNEALGEECAANVFLFYVAGS 300
CYP6Z8_Liv RFVTDIVTKQIEHREKNNVTRKDFQLLIDLRREDNNNEALGEECAANVFLFYVAGS
CYP6Z8_Bora DSTTAVAFTLHELQNVETMKLQTEIDEMLVKTSGLTYDGIKREMSYLDLCKVKELRK 360
CYP6Z8_Liv DSTTAVAFTLHELQNVETMKLQTEIDEMLVKTSGLTYDGIKREMSYLDLCKVKELRK
CYP6Z8_Bora YFGLAILNRETKSYAVPNSNIVLKKGTQVVIPLLAYGMDKEYFPEPDRYLPERFDSTK 420
CYP6Z8_Liv YFGLAILNRETKSYAVPNSNIVLKKGTQVVIPLLAYGMDKEYFPEPDRYLPERFDSTK
CYP6Z8_Bora NYDEKAFYFPGEGPNCIAFRMGVMSKICLVLLLSRFNFEATRGKIFPSTVALLPK 480
CYP6Z8_Liv NYDEKAFYFPGEGPNCIAFRMGVMSKICLVLLLSRFNFEATRGKIFPSTVALLPK
CYP6Z8_Bora GGI PVKISIR
CYP6Z8_Liv GGI PVKISIR
    
```

Figure S2 Alignment of *Ae. aegypti* CYP6Z8 protein sequences

Differences between CYP6Z8 obtained from the genome sequence (AaeGL1.2 geneset, Liverpool strain) and CYP6Z8 cloned from the Bora-Bora strain are shaded. The degree of sequence conservation is indicated by standard motifs. Substrate-binding site regions are indicated by boxes.

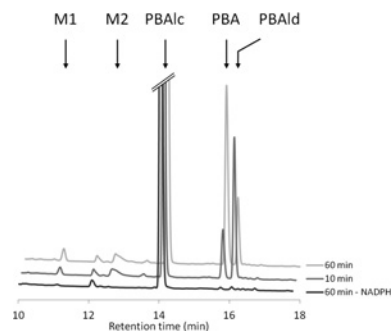


Figure S3 Analysis of PBAIc metabolism by *An. gambiae* CYP6Z2

HPLC chromatograms (off-set) showing the time course of PBAIc metabolism by AgCPR-CYP6Z2 membranes. The lowest off-set corresponds to the negative control (– NADPH) followed by reactions in the presence of NADPH stopped after 10 and 60 min. PBAIc, PBAId, PBA and metabolite peaks are indicated.

¹ To whom correspondence should be addressed (email jean-philippe.david@ujf-grenoble.fr).

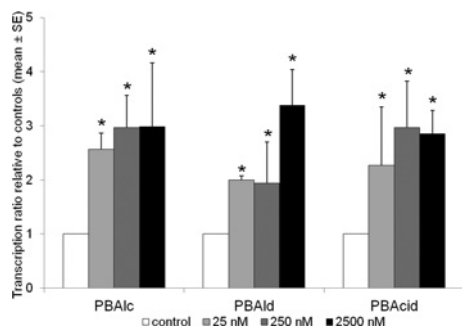


Figure S4 Induction of *CYP6Z8* by PBAIc, PBAId and PBA

Third-stage larvae were exposed for 24 h to three increasing doses of each compound. Transcription levels were measured by qPCR on pools of larvae from three independent replicates and expressed as means \pm S.E.M. relative to controls (unexposed larvae). The significance of transcription ratios relative to controls were assessed by a Mann–Whitney test ($n=3$). * $P < 0.05$.

Table S1 LC–MS analysis of PBAIc and PBAId metabolites

Masses of $[M + H]^+$ ions were measured by HPLC coupled with MS (electrospray positive mode). Theoretical expected mass in this mode, dehydrated mass and observed mass are indicated. –, no dehydration is observed; ?, whether dehydration occurs or not is unknown.

Compound	Theoretical mass	Dehydration (– 18)	Observed mass
PBAIc	201	183	183
PBAId	199	-	199
PBA	215	-	215
M1	Unknown	?	200
M2	Unknown	?	228

Table S2 MS/MS analysis of PBAIc and PBAId metabolites

Fragmentation ions observed in MS/MS (electrospray positive mode) are shown for each compound. Parental ions ($[M + H]^+$) are shown in bold. Common fragments are underlined.

Compound	Observed mass of fragmentation ions														
PBAIc										183		165	<u>155</u>		
PBAId											199		<u>171</u>		
PBA		215											<u>171</u>		
M1											200				
M2	228			211				193		182		175	172	<u>155</u>	151

Received 25 April 2013/10 July 2013; accepted 11 July 2013

Published as BJ Immediate Publication 11 July 2013, doi:10.1042/BJ20130577

Table S3 Docking binding scores

Binding scores of the best ranked poses (kJ/mol) of PBAIc, PBAId, PBA and deltamethrin in members of the CYP6Z family. Ae, *Ae. aegypti*; Ag, *An. gambiae*.

Family	PBAIc	PBAId	PBA	Deltamethrin
AgCYP6Z1	34.49	34.64	31.99	37.24
AgCYP6Z2	37.09	36.46	33.43	42.69
AgCYP6Z3	36.73	36.18	33.69	43.4
AgCYP6Z4	34.22	32.17	31.55	42.76
AeCYP6Z6	34.25	34.43	30.59	45.24
AeCYP6Z8_bora	37.63	35.71	32.28	42.93
AeCYP6Z8_liv	36.34	36.42	31.97	42.55
AeCYP6Z9	31.15	30.6	28.68	41.1